# Toroidal Single Wall Carbon Nanotubes in Fullerene Crop Circles

Jie Han

MRJ, Inc. at NASA Ames Research Center, Moffett Field, CA 64035

han@nas.nasa.gov

## Abstract

*We investigate energetics and structure of circular and polygonal single wall carbon nanotubes (SWNTs) using large scale molecular simulations on NAS SP2, motivated by their unusual electronic and magnetic properties. The circular tori are formed by bending tube (n, n) whereas the polygonal tori are constructed by turning the joint of two tubes of (n, n), (n+1, n-1) and (n+2, n-2) with topological pentagon-heptagon defect, in which n=5, 8 and 10. The strain energy of circular tori relative to straight tube decreases by $1/D^2$ where D is torus diameter. As D increases, these tori change from buckling to an energetically stable state. The stable tori are perfect circular in both toroidal and tubular geometry with strain < 0.03 eV/atom when D > 10, 20 and 40 nm for torus (5,5), (8,8) and (10,10). Polygonal tori, whose strain is proportional to the number of defects and 1/D, are energetically stable even for D < 10 nm. However, their strain is higher than that of perfect circular tori. In addition, the local maxium strain of polygonal tori is much higher than that of perfect circulat tori. It is ~0.03 eV/atom or less for perfect circular torus (5,5), but 0.13 and 0.21 eV/atom for polygonal tori (6,4)/(5,5) and (7,3)/(5,5). Therefore, we conclude that the circular tori with no topological defects are more energetically stable and kinetically accessible than the polygonal tori containing the pentagon-heptagon defects for the laser-grown SWNTs and Fullerene crop circles.*

## 1. Introduction

Fullerene crop circles have been observed in laser-grown single-wall carbon nanotubes (SWNTs) by Liu et al.[1]. These circular types of SWNT ropes, with diameters of 300-500 nm and widths of 5-15 nm, are mostly composed of the tori of individual SWNT with tube diameter of 1.0-1.5 nm. The toroidal nanotube structures are of great interest in their potential novel device applications as they inherit conductivity of, for example, (10,10) metal nanotubes [2-5]. This offers a prototype for studying unusual electronic, magnetic and even superconductivity properties in a ring type of quantum wire with a turning of the current that creates magnetic moment.

Still, the formation and structure of toroidal SWNT is uncertain. It appears that there is no topological pentagon-heptagon defects in the toroidal structures as one hardly finds kinks, created by these defects, along the circumferences of the tori. Thus the formation somehow is similar to the topological construction of the nanotube. That is, the torus is formed by rolling up a straight tube as the tube is generated by rolling over a layer of graphene sheet. It might be a smaller probability for the two ends to come together as compared to bending the nanotube, but such an event will be able to occur through, for example, a growing nanotube eating its own tail, as Liu et al suggested [1].

However, only circular appearance of the toroidal nanotubes seen from scanning force micrograph (SFM) or transmission electron micrograph (TEM) is not enough to rule out the existence of topological pentagon-heptagon defects. Introducing the pentagon-heptagon pairs at the open ends of growing tubes can bend the tube and change its helicity, and eventually form toroidal or helically coiled structures.

Helically coiled multi wall nanotubes (MWNTs) have been frequently observed in the experiments on catalytic decomposition of hydrocarbon and the turning of the tubes are attributed to the introduction of the pentagon-heptagon defects[6]. But the growth mechanism model suggested for the catalytic decomposition process [6] may not suited for the SWNT tori seen from the laser vaporization (LV) approaches as they do not follow the same growth mechanisms of nanotubes[3]. Toroidal nanotubes formed by introducing the pentagon-heptagon defects have been hypothesized. They are actually not circular, but polygonal with 6 or 5-fold rotational symmetry, 12 or 10 straight nanotubes as the toroidal perimeter and 300 or 360 bends as rotational unit [7-10]. Their energetic stability has been studied by the first principle calculations [11]. It was suggested that the circular tori were not as energetically stable as the polygonal tori [10]. However, all the previous work is not appropriate to explain the toroidal structures in the Fullerene crop circles. On one hand, the marked polygonal side features do not agree the circular appearance observed from the SEM and TEM [1]. On the other hand, the system sizes (<2000 atoms or 6 nm in torus diameter) were too small to evaluate the relative stability of the circular tori to polygonal tori. The larger the diameter of the circular tori, more energetically stable. Therefore one can expect the preference of the circular tori over the polygonal tori when their diameters increase to certain values.

In this work, we used the empirical Tersoff-Brenner many body chemical bonding potential [12] to study energetics and structure of circular and polygonal tori of SWNTs. The empirical potential has been shown to be accurate for straight and toroidal carbon nanotubes as compared to first-principles calculations [11]. In addition, it is also computationally accessible to use this potential in studying our current molecular systems up to 30,000 atoms and the torus diameters of 60 nm. All computations were carried out using author's parallel version of molecular simulation code on SP2 at NASA Ames NAS.

## 2. Circular Tori

We started with the circular tori formed by bending tube (n, n) with n=5, 8 and 10 and tube diameter, d=~0.7, 1.1 and 1.4 nm. The laser-grown SWNTs in which the Fullerene crop circles have been observed mostly are the (10,10) metallic tubes. According to the growth mechanism proposed for the LV approaches, the transition metal that co-condenses with the vaporized carbon will prevent introducing pentagon defects from closing the open ends of the tubules. Therefore, one can argue that it is more likely to form defect-free circular tori than polygonal tori incorporated with pentagon-heptagon defects.

One primary question is what is the minimum curvature radius in which a SWNT can be bent to form an energetically stable circular torus. One solution is to use the strain-diameter relationships, as shown in Fig. 1. They were obtained through the energy minimization procedures using Tersoff-Brenner potential. The number of atoms was from ~2000 to ~30,000. The strain energy was defined as the difference in binding energy between the torus and the straight infinite length tube. The energy of the straight nanotube was obtained using periodic boundary conditions on two ends of the tube of length at about 6 nm. The torus radius was averaged distance between all the atom positions and torus mass center. As expected, the strain energy is a decreasing function of the torus diameter, D. Several features of strain-diameter curves are shown in Fig. 2, taking torus (8,8) as an example.

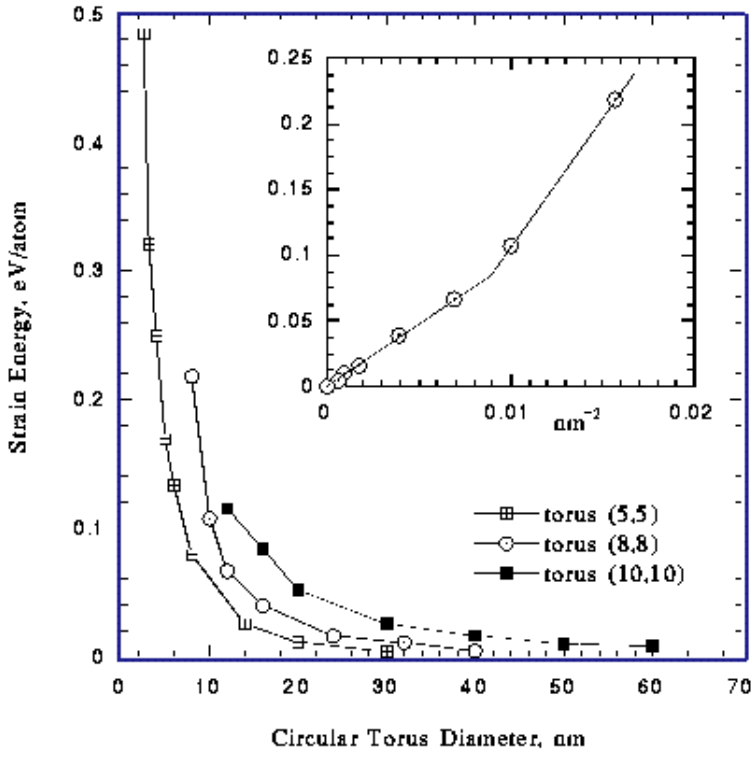



*Fig. 1. Strain energy per atom of circular tori relative to straight tubes as functions of torus diameter, D. The insert shows a linear relation between the strain energy and $1/D^2$ for torus (8, 8). The turning point represents a transition from buckling in higher energy to perfect circular tori in lower energy. Reference energy is -7.2513, -7.3231 and -7.3482 eV/atom for straight infinite length tube (5, 5), (8, 8) and (10, 10)*

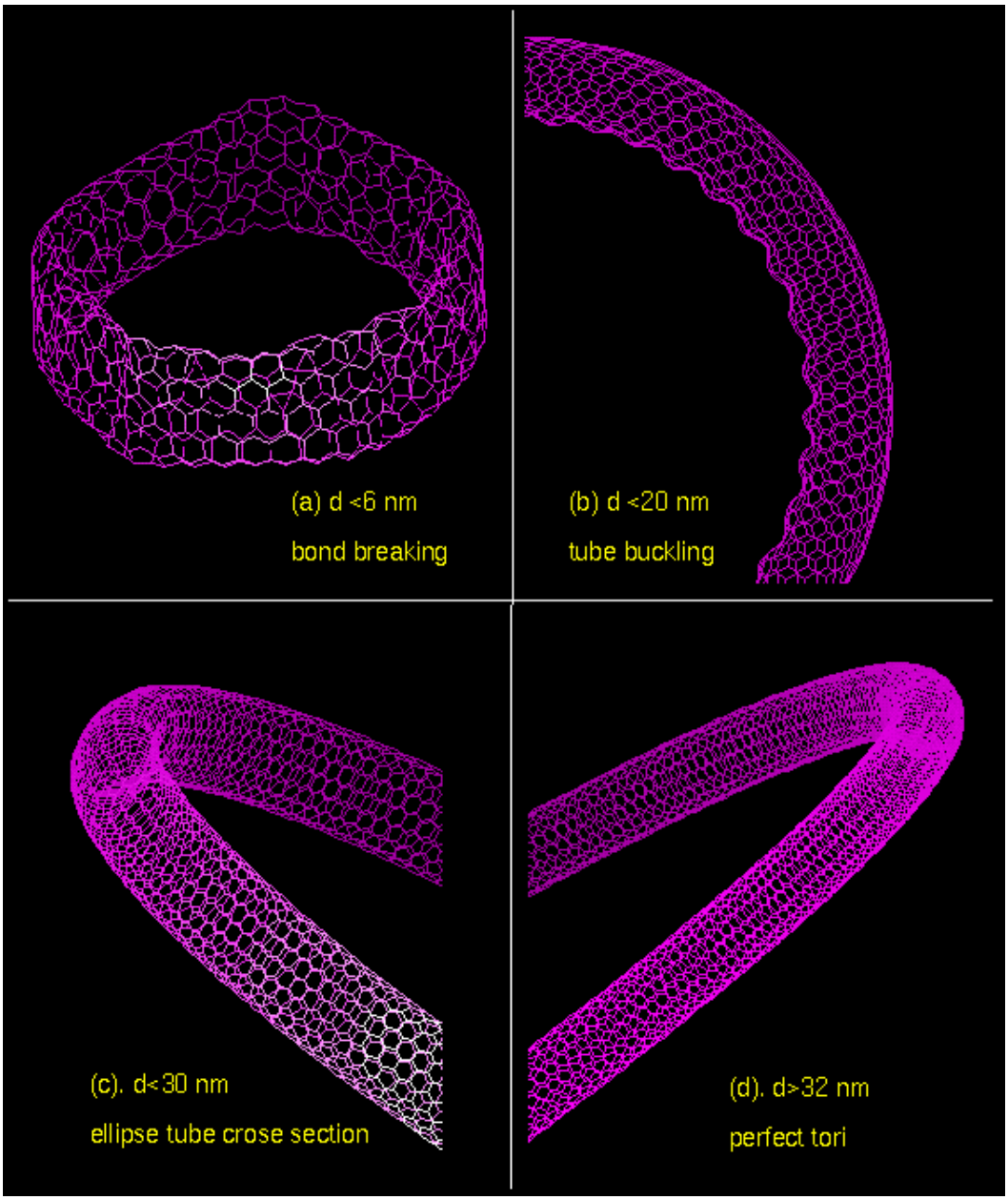



*Fig. 2. Configurations of circular torus (8,8) in different ranges of torus diameters*

For D < 6 nm, very high strain (the values are not shown in Fig. 1) breaks C-C bonds; for 10nm > D < 20 nm, the toroidal tube keep buckling. In this case, no energy minima were found as energy gradients were oscillatory around 0.03 - 0.10 eV/Å/atom and the buckling positions keep migration (0.001 eV/A/atom was taken as convergent criterion in this work). The migration is due to existence of a number small barriers corresponding to kinks. The energy values in this case shown in Fig. 1 were the averages over period of oscillation. As the torus diameter increases, bending strain is alleviated and buckling disappears. After a transition in which the tube cross section appears ellipse, the tori seem perfect circular even in tube cross section and become energetically stable when D>10, 20 and 40 nm for torus (5,5), (8,8) and (10,10), respectively. Such tori are called perfect circular tori in this work. Since there is no clear distinction between ellipse and circular tubular cross section, these critical values, in

which tubular torus is considered to be energetically stable, are rough estimations. It is interesting to note that the strain energy is less than 0.03 eV/ atom for all the perfect tori.

The strain energy per atom of circular tori was found to be a linear function of $1/D^2$. This is also illustrated in Fig. 1 for torus (8,8). It has been well known the tube strain energy per atom relative to the graphene sheet is proportional to $1/d^2$ where d is the tube diameter [13]. From energetic point of view, bending a straight tube is similar to bending a planar sheet. Beyond the elastic limit of tube, bending leads to buckling. The critical diameter for buckling was found in this work to be ~6, 16 and 30 nm for tube (5,5), (8,8) and (10,10). A generalized correlation for the buckling curvature of tubes of diameter between 1.0 to1.5 nm [14] gave ~8.5 and 14.0 nm for tube (8,8) and (10,10), in agreement with our observations to the circular torus considering the uncertainity in determining buckling curvature.

We also defined and calculated the local maximum strain as the energy difference between the energy maxima at atom positions of the torus and the energy of corresponding straight tube. This strain is an indicator of kinetic barrier of tube bending. For perfect circular tori, the value was found to be stightly larger than the averaged strain by a factor of 1.0-1.1. This shows uniform strain distribution over all the atoms in perfect circular tori. The thermal energy at LV temperature (1200°C) is about 0.1 eV/atom, as compared to the strain of <0.03 eV/ atom in perfect circular tori. We can see that thermal energy is responsible for, at least partly, driving SWNTs to form perfect circular tori. The SWNT bends with radii of curvature of tens of nm have been frequently observd. The circular tori with diameter at 100 nm was also seen more recently. When D>100 nm for torus (10,10), the strain energy of circular tori is less than 0.01 eV/atom, according to the strain dependence of $1/D^2$.

### 3. Polygonal Tori

The laser-grown SWNTs also contain smaller amounts of (11,9) and (12,8) as well as (10,10) tubes [15]. This opens possibilities to form polygonal tori. If the topological defects were introduced into the open ends of a growing tube and survive, the tube would change its helicity and form the joint of tubes with different helicities. Shown in Fig. 3 are the joint models of tube (10,10), (11,9) and (12,8). Joint (11,9)/(10,10) or (12,8)/(11,9) has only one defect and configuration with the bent angle of ~40. In contrast, joint (12,8)/(10,10) has two defects and at least two configurations (a) and (b) with the bent angles of ~18° and ~0°, respectively. The small angle bend models were also proposed for heterojunction devices by Chico et al [16]. Their (8,0)/(7,1) and (8,0)/(6,3) joints contain one and three fused pentagon-heptagon defects with the bent angle between 0-15°. Similar joint models were also constructed from the (5,5), (6,4) and (7,3) tubes in this work.

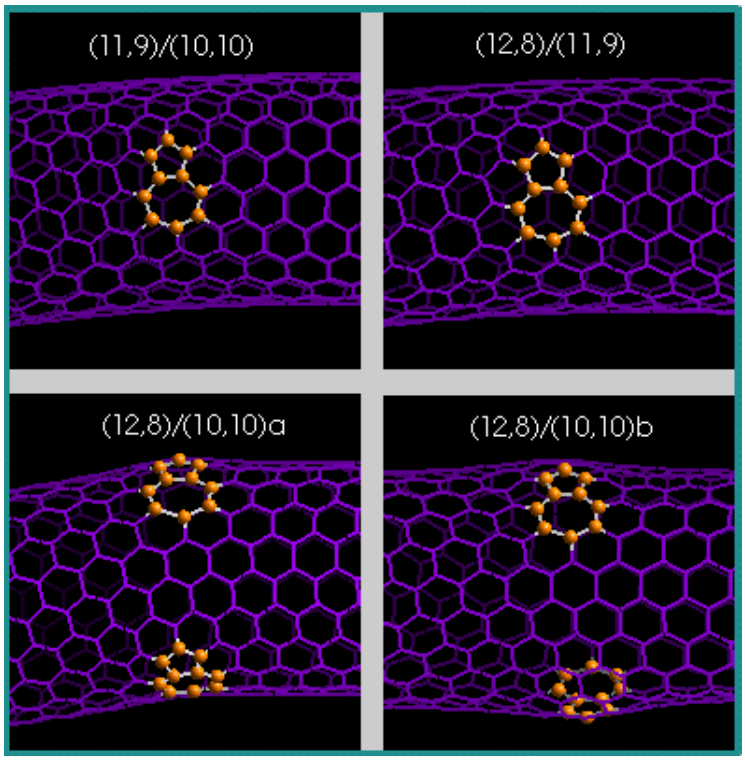



*Fig. 3. Joint configurations. The (11, 9)/(10, 10) and (12, 8)/(11, 9) only need one fused pentagon-heptagon defect to form ~4° bends while they are semiconductor/metal and semiconductor/semiconductor heterojunctions, respectively. The (12, 8)/(10, 10) need two defects and therefore could have at least two configurations, depending on the arrangements of defects.*

Two polygonal tori made from the joints are shown in Fig. 4. Torus a is formed by a 6-fold rotation of joint (5,5)/(9,0)/(5,5) of two 30° bends as a scale up model of the previous ones [7-11]. Obviously, it looks unlike the observed tori in ref. 1. Torus b is formed by 30-fold rotation of joint (5,5)/(6,4)/(5,5) of two 6° bends. As the bent angle decreases or the number of sides of the polygonal torus increases, the polygonal torus approaches circular torus. Therefore,

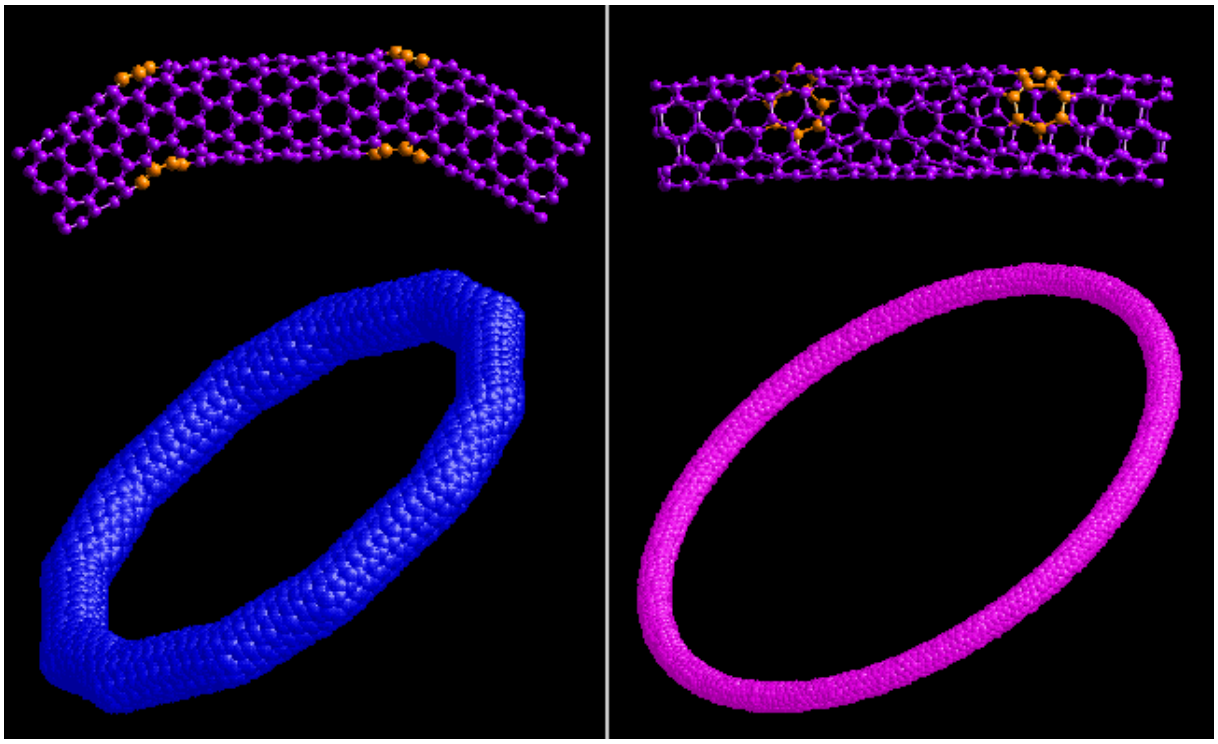


*Fig. 4. Polygonal tori and joints as construction units. The left torus is formed by a 6-fold rotation of joint (5,5)/(9,0)/(5,5) with bend angle of 30°. The right torus is formed by a 30-fold rotation of joint (5,5)/(6,4)/(5,5) with bend angle of 6°. Note that both tori have the same tube diameter and different torus diameter.*

the torus (6,4)/(5,5) looks like a circular torus. The bent angle, 30°, is not optimized geometry. The optimized value was found to be ~33° for joint (18,0)/(10,10) and ~36° for joint(9,0)/(5,5) in this work. The semiempirical CNDO calculations also gave the value of ~36° for joint (9,0)/ (5,5) [17]. It can be expected that the bent angle approaches 30°, Dunlap's 2D projection value [8], as tube diameter increases. Thus the optimized (5,5)/(9,0) torus should be made of the 36#176 bends and have 5-fold symmetry. The polygonal tori would be perfect if the 180° was the integer multiple of the bent angle. In this case, the tube keeps straight and the torus strain is only around the defects. The most polygonal tori, however, are not perfect. In this work, we chosen the bent angle close to the optimized value for forming the polygonal tori. For example, the 6° instead the optimized ~7° joint was used to obtain the (6,4)/(5,5) torus. The size of torus with given angle varies by changing the length of straight tube.

The strain energy of some polygonal tori was shown in Fig. 5. The reference energy was taken from that of infinite length straight tube (n, n) as was done for the circular tori. The torus radius was the average distance between all the atom positions and the torus mass center. The total strain energy of the polygonal tori is proportional to the number of the defects (the pentagon-heptagon pairs) while the strain per atom is proportional to 1/N (N, number of atoms) or 1/D if the tube bending strain is ignored. Thus two features can be seen from Fig. 5. The strain energy is lowered from torus (6,4)/(5,5) (60 defects) to (7,3)/(5,5) (40 defects) while torus (9,0)/(5,5) of diameter at only ~7 nm (2112 atoms, 12 defects) is only at very small strain of 0.016 eV/atom. On the other hand, the strain energy of polygonal torus, for example, (7,3)/(5,5), is lower in the range of small diameters and higher in the larger diameters than that of circular torus (5,5). This is because the strain energy per atom is proportional to $1/D^2$ for the circular tori and 1/D for the polygonal tori (see the inserted figure in Fig. 5). The observation that the strain of

polygonal torus is a linear function of 1/D implies that the tube bending (~D°) can be ignored compared to dominant contribution of the defects to the total strain in the polygonal tori. In general, the strain energy of polygonal tori is larger than that of perfect circular tori if they are composed of (n, n), (n+1,n-1) and/or (n+2, n-2). Lower strain of polygonal tori relative to circular tori, however, can be reached for smaller diameter or high bent angle structure such as (9,0)/(5,5).

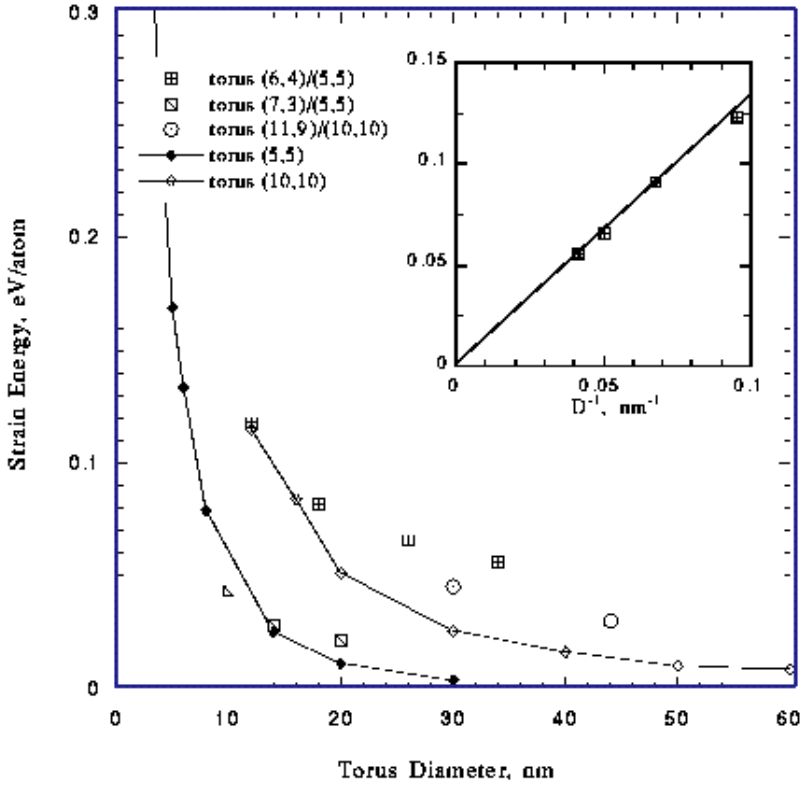



*Fig. 5. Strain energy per atom of tori relative to straight tubes as functions of torus diameter, D. The inserted figure shows a linear relation between the strain energy and 1/D for polygonal torus (6, 4)/(5, 5). Reference energy are the same for circular and polygonal tori, as given in Fig. 1.*

The averaged strain per atom will be zero in both circular and polygonal tori if D goes to infinity. For circular tori, this means that strain disappears both globally and locally since the strain is evenly distributed. For polygonal tori, however, the defect strain remains the same. Therefore, the averaged strain per atom is not sufficient and local maximum strain should be added. The local maximum strain was found to be 0.13 eV/atom for torus (6,4)/(5,5), localized at one pentagon-heptagon defect and 0.21 eV/atom for torus (7,3)/(5,5), localized at two pentagon-heptagon defects. It slightly changed to 0.11 eV/atom for torus (11,9)/(10,10). Compared to them with lower thermal energy, 0.10 eV/atom at 1200°C, one concludes that these defects hardly survive even though they can be formed in LV process [2].

**4. Concluding Remarks**

We carried out extensive molecular mechanics calculations for circular and polygonal tori. The total

strain energy and local maximum strain energy results prefer perfect circular tori to polygonal tori while both of them are energetically stable for the torus diameter over certain critical values. This supports the hypothesis that defect-free circular SWNT tori are dominant constituents of the observed Fullerene crop circles in laser-grown SWNTs [1].

The strain energy per atom is not sufficient for identification of the energetic stability of carbon cage structures if the strain distributions are not evenly distributed over all the atom positions. Therefore, we suggested the local maximum strain for the structure identification. The local maximum strain can be considered as the kinetic barrier to the formation of local structure. The strain energy per atom relative to graphite is higher for the C60 than C70 and higher fullerenes [17]. However, it is C60 that has highest stability from both kinetic and energy point of view. This is because the strain energy is most evenly distributed over each atom and the local maximum strain reaches lowest in the highest symmetry C60 out of all the fullerenes. Similarly, the circular tori are more energetically stable and kinetically accessible than the polygonal tori because the total strain or local maximum strain in the circular tori is evenly distributed over torus circumference and gets effectively released as the bent tube is lengthened. We would argue that the work that used the strain energy per atom relative to C60 for evaluations of relative stablility of carbon cage structure, including polygonal tori relative to C60, is questionable, or at least incomplete.

We also wish to emphasize that our preference of the circular tori over the polygonal tori in this work is specific for the laser-grown SWNTs. In carbon nanotubes grown on catalytic particles through catalytic decomposition of hydrocarbon, the existence of joint structure has not been ruled out. In fact, the observed helically coiled MWNTs have been hypothetically attributed to the joints of tubes with different helicities. The observation that radius of the coiled MWNTs of diameters>2 nm was down to 16 nm [6] and our calculations that shows a tube of diameter of 1.4 nm cannot be bend to form stable coil of diameter < 20 nm, in fact, rule out possibility of the helically coiled nanotubes being formed by bending same helical tubes without topological defects. Our additional calculations have shown that SWNTs can stay in stable coiled or toroidal states only if topological defects are incorporated, as one can expects. A most recent study suggested that the turning of MWNTs be resulted from competition between curvature elasticity and interlayer adhesion in the catalyst-grown MWNTs [17]. That is, the van der Waals interactions between interlayers stabilize the tube turning. However, the turning must be also related to catalyst particles since helically coiled MWNTs have been seem only from the catalyst-grown approaches not such catalyst-free arc methods [6]. If the catalysts do stabilize the topological pentagon-heptagon defects, it is likely to observe joint structures from the catalyst particle-grown SWNTs.

**References**

1. J. Liu, H. Dai, J. H. Hafner, D. T. Colbert, S. J. Tans, C. Dekker,and R. E. Smalley, Nature, 385, 780 (1997)

2. A. Thess, R. Lee, P. Nikolaev, H. Dai, P. Petit, J. Robert, C. Xu, Y. H. Lee, S. G. Kim, D. T. Colbert, G. Scuseria, D. Tomanek, J. E. Fischer, and R. E. Smalley, Science, 273, 483 (1996)

3. H. Dai, A. Rinzler, P. Nikolaev, A. Thess, D. T. Colbert, and R. E. Smalley, Chem. Phys. Lett. 260, 471 (1996).

4. S. J. Tans, M. H. Devoret, H. Dai, A. Thess, R. E. Smalley, L. J. Geerlings, and Cees Dekker, Nature,

386, 474 (1997)

5. J. E. Fischer, H. Dai, A. Thess, R. Lee, N. M. Hanjani, D. DeHaas, and R. E. Smalley, Phys. Rev. B.55, 4921 (1997)

6. S. Amelinckx, X. B. Zhang, D. Bernaerts, X. F. Zhang, V. Ivanov, and J. B. Nagy, Nature, 265, 635, 1994; X. F. Zhang and Z. Zhang, Phys. Rev. B.52, 5313, (1995)

7. B. I. Dunlap, Phys. Rev. B.46, 1933 (1992)

8. L. A. Chernozatonskii, Phys. Lett. A170, 37 (1992)

9. S. Itoh, S. Ihara, and J. Kitakami, Phys. Rev. B.47, 1703 (1993), B. 48, 5643 (1993), B.48, 5643 (1993); S. Itoh and S. Ihara, Phys. Rev. B.48, 8323 (1993), B.49, 13970, (1994)

10. B. Borstnik and D. Lukman, Chem. Rev. Lett. 228, 312, (1994)

11. J. K. Johnson, B.N.Davidson, M. R. Pederson, and J. Q. Broughton, Phys. Rev. B 50, 17575, (1994)

12. D. W. Brenner, Phys. Rev. B 42, 9458 (1990)

13. D. H. Robertson, D. W. Brenner, and J. W. Mintmire, Phys. Rev. B 45, 12593 (1992)

14. S. Iijima, C. Brabec, A. Maiti, and J. Bernholc, J. Chem. Phys. 104, 2089 (1996)

15. J. M. Cowley, P. Nikolaev, A. Thess, and R. E. Smalley, Chem. Phys. Lett. 265, 379 (1997)

16. L. Chico, V. H. Crespi, L. X. Benedict, S. G. Louie, and M. L. Cohen, Phys. Rev. Lett., 76, 971 (1996)

17. A. Fonseca, E. A. Perprete, P. Galet, B. Champagne, J. B. Nagy, J-M Andre, Ph Lambin and A. A. Lucas, J. Phys. B 29, 4915 (1996)

18. A. Maiti, C. J. Brabec, and J. Bernholc, Phys. Rev. Lett. 70, 3023 (1993)

19. O-Y. Zhong-can, Z-B. Su and C-L. Wang, to appear in Phys. Rev. Lett.